

On Deep Generative Modeling in Economics: An Application with Public Procurement Data

Marcelin Joanis¹, Andrea Lodi^{1,2} and Igor Sadoune*¹

¹Department of Mathematics and Industrial Engineering, Polytechnique Montreal, Montreal, QC, Canada

²Jacobs Technion-Cornell Institute, Cornell Tech and Technion - IIT, New York, NY, USA

Abstract

We propose a solution based on deep generative modeling to the problem of sampling synthetic instances of public procurement auctions from observed data. Our contribution is twofold. First, we overcome the challenges inherent to the replication of multi-level structures commonly seen in auction data, and second, we provide a specific validation procedure to evaluate the faithfulness of the resulting synthetic distributions. More generally, we argue that the generation of reliable artificial data accounts for research design improvements in applications ranging from inference to simulation crafting. In that regard, applied and social sciences can benefit from generative methods that alleviate the hardship of artificial sampling from highly-structured qualitative distributions, so characteristic of real-world data. As we dive deep into the technicalities of such algorithms, this paper can also serve as a general guideline in the context of density estimation for discrete distributions.

Keywords : discrete deep learning, generative adversarial networks, variational autoencoders, simulations, public procurement

1 Introduction

In recent decades, new avenues to statistical modeling have emerged from advances in computer science. Despite conflicting philosophies and goals, machine learning techniques are finding their place in economics, and provide a methodological framework that adapts to contemporary datasets such as satellite imagery, texts or high-dimensional data [1, 2]. In contrast, here we explore another aspect of deep learning that may be less popular outside the sphere of computer science, namely *deep generative modeling* (DGM) or *deep generative models* (DGMs). Deep generative modeling refers to a set of methods that intend to perform density estimation using *artificial neural networks* (NNs) as function approximators. Some DGMs are able to capture an explicit representation of the targeted joint distribution, while others only offer an implicit (“black box”) form of it. The former family of methods can be used for inference, sampling or both at the same time, while the latter only provides ways to sample, but with the benefit of being portable, easier to use and less computationally demanding. In this study, we will linger on the two most popular and studied algorithmic architectures used for sampling, namely the *generative adversarial networks* (GANs) [3] and the *variational*

*Corresponding author.

E-mail addresses: marcelin.joanis@polymtl.ca (M. Joanis), andrea.lodi@cornell.edu (A. Lodi), igor.sadoune@polymtl.ca (I. Sadoune).

autoencoders (VAEs) [4] frameworks. Although VAEs are technically explicit estimators, they are actually similar to GANs in their benefits and goals. In general, DGM emerges as a powerful tool supporting empirical investigations by offering ways to perform data augmentation, balancing and replication, but also carries the potential to have a profound impact in social sciences. Indeed, we can envision that by powering agent-based simulations, DGMs will render game-theoretic computational experiments more attractive, and in a general way, will invigorate the *complex system* approach.

1.1 Deep generative modeling in social sciences

The goal of DGM is to generate (virtually) infinite sequences of data points from a limited number of empirical observations, with no particular knowledge of the data structure being required [5]. In other words, one can replicate and sample from an empirical distribution without pre-existing model of its data generation process. GANs, in particular, have proven to be a huge success in this endeavor [6], but mainly within the scope of native applications (i.e., imagery or natural language processing [7]). Although DGMs are still underused in social sciences, they can potentially provide substantial improvements in any application relying on qualitative data, and they already have proven to be useful for:

Data amplification. High-dimensional data are commonly associated with low degrees of freedom, impairing regression or classification analysis. Data generation allows to amplify the number of observations, and thus helps with high-dimensional or small datasets. DGMs can also amplify weak signals within categorical configurations, as shown in [8], where the authors offset unbalances in a credit card dataset. Other examples are found in the medical field, where GAN-based data amplification is now popular for recovering patient characteristics from partial information [9].

Privacy. The use of synthetically generated data makes a lot of sense when privacy is an issue, as it is often the case when working with medical or financial data. Although GANs find naturally their place in this endeavor, a specialized literature has recently emerged, as privacy entails a unique challenge [10].

Counterfactual and causal learning. DGMs can be used for the estimation of unseen or partially unseen distributions. For example, a GAN-based model is assigned to the task of generating counterfactual proxies in [11]. In the same vein, in [12] and [13], VAEs are used in order to estimate the latent structure of causal graphs that, in turn, serve as oracles to infer causal effects.

Simulations. The complex system standpoint emerged in the late 20th century as a tendency to represent economic mechanisms from an inductive perspective [14]. However, this approach relies on computer simulations that are traditionally based on a set of hard-coded rules and stylized facts, raising realism issues. In addition, simulations often require large amounts of development time and computing resources [15], and since the empirical shift in economics intensified during the digital era [16], the simulation approach has lost some traction. However, machine learning techniques create the opportunity to make agent-based modeling (ABM) an attractive research design to represent social behaviors in economics [17]. We argue that DGMs could and should play a crucial part in the development of ABM. Indeed, a generator of synthetic data can act as an independent module that can be plugged to already existing simulations or systems, or be used to generate standalone realistic artificial environments. Furthermore, DGMs can easily be updated if new data are available, hence preserving the realism of a simulation through time. For example, in [18], the authors provide a large-scale simulation of travel behaviors generated from real-world data using *restricted Boltzmann machines* [19]. The same goes for time series, GANs being used to sample realistic financial correlation matrices [20], or financial time-series [21].

1.2 The case of Public Procurement

The public procurement (PP) problem is the one of supplier selection by public authorities, or more generally the problem of how to efficiently allocate public funds in exchange for goods and services. Despite the existence of several designs for supplier selection [22], PP efficiency is a long-standing problem and is still impaired by collusion [23]. The minimum price rule is the choice of most western economies for its simplicity and because it is believed to preserve competition, regardless critics and failures [24]. The problem of collusion has traditionally been tackled empirically, and we denote successful attempts to detect collusive activities using econometrics. Recently, the PP problem got some attention with the appearance of *tacit* (or algorithmic) collusion. This type of collusion arises from the increasing use of automated pricing by the private sector, and does not reflect a clear criminal endeavor, but rather seems to be caused by algorithmic convergence [25, 26, 27, 28, 29]. Accordingly, DGM seems to shed light on new perspectives for the PP research, and, by extension, for the study of market mechanisms. As alluded earlier, DGMs could be used to power realistic agent-based market simulations. This is an already popular approach in the study of electricity auction markets, where simulated environment based on hard-coded rules are used [30, 31, 32, 33, 34]. However, PP data are defined by characteristics that challenge deep learning methods when it comes to density estimation and sampling. In this study, we dive deep into the technicalities inherent to the sampling of fake but realistic auctions from public procurement data using discrete deep learning.

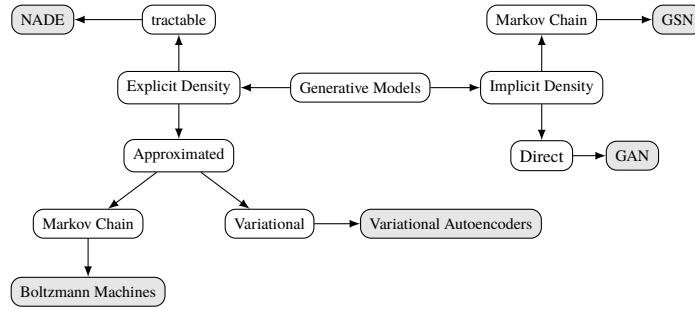
1.3 Paper Organization

Section 2 provides a short account of deep generative modeling, and formally introduces the methods that are used throughout this study. Section 3 discusses the challenges inherent to the use of DGMs, and in particular of GANs, with high-dimensional qualitative data. Section 4 describes and formalizes the solution to the problem raised in this study, namely the generation of synthetic public procurement data. Section 5 provides a validation procedure for the artificially-generated data and reports all the important results of the study. Finally, Section 6 offers a post-experiment discussion on the use of DGMs for public procurement research, economics and applied sciences.

2 Background

Deep generative methods follow deep learning principles in order to approximate multi-dimensional probability functions. Those techniques are often preferred to their classical counterparts (e.g., Bayesian models) because they do not require a prior knowledge of the data structure of interest. Nevertheless, it is true that some DGMs are designed in a way that allows, or even encourages, the encoding of prior knowledge. For example, the *Neural Autoregressive Density Estimator* (NADE) [35] is a tractable approximator of discrete distributions that can work with a specified variable ordering. Figure 2.1 classifies DGMs according to their ability, or inability, to approximate a tractable functional form. Typically, explicit approximators provide the estimated parameters of the targeted distribution, and hence bring a tractable solution to the problem of density estimation. The main advantage of such methods is that once the joint probability function is known, then virtually any question can be answered. It follows that the tractable (or explicit) estimators can perform both sampling and inference. In contrast, implicit methods rely on relatively lightweight black-box algorithms that are more robust to complexity (e.g., mixed data type, multi-level, high dimension) but specialized in sampling.

Figure 2.1: Taxonomy of deep generative models, adapted from [36, Figure 9].



2.1 Generative Adversarial Networks

The idea of *adversarial learning* is rooted in game-theoretic principles. Indeed, the *generator* G and the *discriminator* D oppose each other in a *minmax game*. The role of D is to assert the probability of its input of being authentic. Let $x \sim p_{real}$ be a data-point of the original dataset. If $D(x) = 1$, then the discriminator rightfully classifies (with certainty) x as an instance of the observed dataset. Its adversary G , samples fake data $\tilde{x} \sim G(z)$ from its input noise variable z , which is drawn from an arbitrary prior distribution p_z (e.g., $z \sim U(0, 1)$). Note that the size of z can be arbitrary, but $G(z)$ must match the dimension of x . The game is represented by the following objective:

$$\min_G \max_D V(D, G) = E_{x \sim p_{real}} [\log(D(x))] + E_{z \sim p_z} [\log(D(G(z)))]. \quad (1)$$

The discriminator maximizes (1) by scoring $D(x)$ close to 1 and $D(\tilde{x})$ close to 0, while the generator minimizes (1) by sampling \tilde{x} such that $D(\tilde{x})$ is close to 1. Since G never interacts with the real data, the optimization of D and G must take place in a synchronized way in order to avoid overfitting. To that end, the hyperparameter $k > 0$ is set as the number of training steps to be executed by D after each training step of G . The learning is expected to end when D is no longer able to discriminate between real and fake samples, i.e., when $D(\tilde{x}) \approx D(x) \approx \frac{1}{2}$. In such case, G generates realistic fake data-points provided that D is not a bad classifier. The main difficulty in training GANs emerges from the fact that there is no unique equilibrium. For instance, if D classifies with a striking accuracy and that G is a bad synthesizer, or more generally if G is too weak compared to D , then the optimization process gets jammed (e.g., *mode collapse* [37]). For optimal results, D and G are represented by neural networks in practice [3]. The graphical representation of vanilla GANs architecture can be found in Figure 2.2.

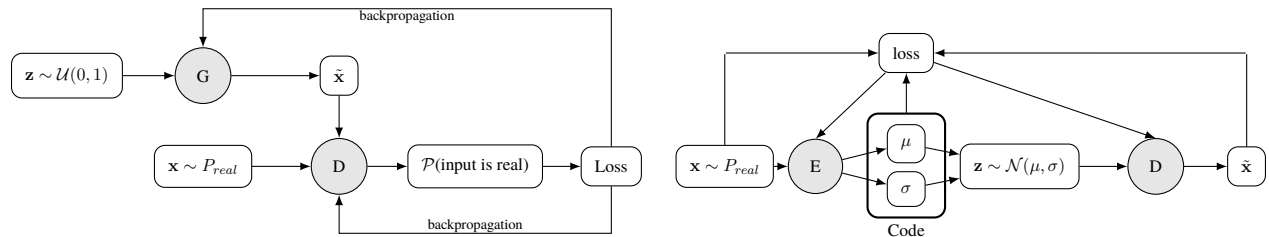
2.2 Variational Autoencoders

An autoencoder, given an input x , is composed of an *encoder* $E : x \rightarrow z$ and a *decoder* $D : z \rightarrow \tilde{x}$, where z is referred as the *code*. In other words, autoencoders can perform nonlinear factor reduction and reconstruction in a nontrivial way so that new samples are generated. Variational autoencoders rely upon *variational inference* [38]—a convenient alternative to *Markov chain Monte Carlo*—in order to approximate the targeted probability function. More precisely, VAEs work by reshaping the code into two independent layers μ and σ that capture the mean and the variance of each dimension of the encoder’s output. Then, a latent signal z is sampled from $\mathcal{N}(\mu, \sigma)$. The decoder approximates $q(z|x)$, while E approximates $p(x|h)$, where h is the last layer of the NN representing the encoder. The parameters of E and D are optimized with respect to

$$\|x - D(z)\|^2 + KL(\mathcal{N}(\mu_x, \sigma_x), \mathcal{N}(0, I)), \quad (2)$$

where KL refers to the *Kullback Leibler divergence*. Provided arbitrarily powerful learners, the VAEs are shown to have zero approximation error [39]. That is why, as with GANs, the encoder E and the decoder D are both represented by neural networks. Figure 2.2 graphically shows how variational autoencoding differs from adversarial learning.

Figure 2.2: Chart of adversarial learning (left) and variational autoencoding (right).



3 Challenges of Using DGMs with Discrete Distributions

In this section, we review the properties of data representing economic and social interactions that make the training of DGMs, and of GANs in particular, more difficult. The discrete nature of such data is at the origin of most of the challenges we are about to describe. To avoid any ambiguity, we note that we define a discrete variable as a categorical space whose values are states. A variable is considered continuous if its set of unique values is large enough, otherwise discrete in the sense we have just defined.

Discrete data and mixed data type. Most real-world datasets are composed of discrete and continuous components. Unfortunately, vanilla deep generative methods do not thrive on discrete inputs which may cause differentiation issues. In addition, discrete and continuous variables must be reconstructed on their original spaces so as the statistical link is preserved.

Multimodal and/or non-Gaussian distribution. Continuous distributions in qualitative datasets are often either non-Gaussian or multimodal. Data synthesizers being sensible to the quality of their inputs, a proper pre-processing of the continuous signals must be applied. It follows that continuous variables will be synthesized according to their modified forms, and hence one must keep in mind that a retro-processing may be needed.

High-cardinality discrete variables. DGMs are sensible to the representation of the discrete variables. Indeed, if a sparse encoding is used on a high-cardinality discrete space, then a naive algorithm could make decisions based on the sparsity of an observation instead of its intrinsic characteristics. On the other hand, if a dense and continuous encoding is used, then it may be difficult to restore the original discrete representation from the synthetic data. For example, if the encoding in question is deterministic (e.g., *categorical embedding* [40]), then it would not be possible to apply the reverse mapping to the generator’s output because of the stochastic nature of the generation process. However, this might not be a problem if the generated data do not need to be interpreted.

Multi-class and multi-label variables. By *multi-class* we refer to binary variables and their generalization in higher dimension, that is, discrete variables that take exactly one value at a time. In contrast, *multi-label* variables potentially encode more than one state in a given instance. For example, the firms in public procurement data can be represented by a multi-label space since several bidding firms are associated with each auction. For a fixed number of instances, the higher the cardinality, the less a particular value of a discrete variable is likely to be observed. This is true for multi-class and multi-label variables, but cardinality is even more punishing in the latter case. Indeed, the number of combinations to a multi-label variable is an exponential function of the number of individual states. The problem can therefore quickly become

intractable.

Unbalanced data. It is not uncommon to find low frequency signals in qualitative datasets, nor it is unnatural. Indeed, unbalanced does not mean incomplete, however, low frequency signals imply scarce training opportunities. The issue raised by unbalanced data echoes the main limitation of any statistical method—the sensibility to the amount of data available.

Validation. The problem of evaluating the reliability of a synthesizer’s output is often answered with domain specific rules. In computer vision, for instance, the validation can be done visually. In the general case, *inception scores* [36, 41] can be used. The term “inception” refers to the idea of using synthetic data as training ground for exogenous classifiers or regressors: a predictor trained on the synthetic data should perform well on a test set composed of real data points. The downside of such procedure is that more models must be trained, and in doing so, one may face the set of difficulties that has motivated this discussion in the first place.

3.1 Training GANs with Discrete Data

A pleiad of accommodations and tricks have been recently proposed to improve GANs stability and performances, but here we concentrate on the most important innovations that relate to the handling of discrete inputs with GANs.

Critic. The *Wasserstein GAN* (WGAN) [42, 43] and the *least-square GAN* (LSGAN) [44] replace the discriminator by a *critic* that no longer classifies, but instead predict how far a given point is from the decision boundary that separates (alleged) real and fake samples. Using a critic has the advantage to penalize samples that lie far from the decision boundary even though they are on the proper side, improving the quality of the signal send to the generator during the optimization process.

Loss functions. The WGAN became one of the most popular GANs architecture. Intuitively, the *Earth Mover* (EM) or *Wasserstein-I* loss measures the distance between the distributions of real and fake samples, in terms of how much “mass” needs to be transported from one to the other. More precisely, the Wasserstein-I distance indicates the cost of the optimal transport plan. What makes the WGAN so attractive is that the critic can be trained to optimality, and the EM loss promotes a stable and robust training.

Policy gradient. Beyond the choice of the loss function, the optimization process itself can be modified. This is the idea of the *boundary-seeking GAN* (BGAN) [45], where the generator is trained according to a policy gradient, allowing discrete and continuous inputs, and promoting a smooth training.

Training by sampling. The *conditional tabular GAN* (CTGAN) [46] is a framework intended to help with data imbalances and discrete inputs. The CTGAN does not provide a specific way to adversarial learning, but rather a meta-algorithm that could be combined with any loss function, network topology or optimization process. The core idea of the CTGAN—*training by sampling*—is to select a discrete variable with equal probability, then to select a state according to the probability mass function of the given variable, and finally to execute a training step using examples that respect the given constraint. Consequently, the generator’s input space is augmented with a conditional vector that encodes the selection.

3.2 Particularities of Public Procurement Data

Our data is derived from the *Système électronique d’appel d’offre* (SEAO)¹ dataset, and is composed of 119,029 contracts offered in public market auctions in the Canadian province of Quebec during the course of ten years (2010-2020). Auction data are defined by a multi-level structure that arises from the association of multi-class and multi-label variables. In our case, the firms are represented by a multi-label variable

¹Organism in charge to record public procurement data in the Canadian province of Quebec.

(firms), and diverse features of the contracts offered are encoded with multi-class variables. Therefore, a given instance is composed of a discrete space that includes auction features, and a set of bidding firms whose size varies from an auction to another and that is associated with a set of continuous bids.

Table 1: Structure of the data. Only competitive open auctions (*number of bidders* > 2) have been considered.

Variables	Type	Cardinality	Count
Discrete	multi-class	6,749	9
	multi-label	40,659	1 (<i>firms</i>)
Continuous	-	-	1 (<i>bids</i>)

Table 1 summarizes the main characteristics of the data, and highlights the problematic nature of the multi-label variable *firms*. Indeed, with a cardinality representing 34% of the number of examples, we cannot hope to achieve an accurate approximation of a joint distribution including such a huge combinatorial structure, at least not in a straightforward way.

4 Generating Synthetic Public Procurement Auctions

An instance of public procurement auction is labeled $a \in \{1, \dots, N\}$, where N is the number of examples. Let C be a collection of multi-class variables representing the features of the contracts being offered. Let $nb \in C$ be the number of bidders to an auction. We adopt a sparse *onehot* encoded form of our discrete space, meaning that each $c \in C$ is represented by a binary vector such that $\sum_i c(i) = 1$, and \mathbf{c} is the aggregated vector of multi-class variables such that $\sum_j c(j) = |C|$. The variable *firms* is now represented by the binary variable \mathbf{f} , such that $\sum_i \mathbf{f}(i) = nb^a$ for each instance a . Thus, an auction a is given by the set $\mathbf{x} = \{\mathbf{c}^a, \mathbf{f}^a, \mathbf{b}^a\}$, where \mathbf{b} is an array of continuous bids. It follows that the number of element in \mathbf{b}^a equals nb^a . Let a^* be an hypothetical auction with only one feature ($|C| = 1$), and two bidders among four firms composing the market. Then, $nb^{a^*} = 2$, and \mathbf{x}^{a^*} could be (depending on which firms are actually bidding) $\{[1, 0], [1, 1, 0, 0], [b_1, b_2]\}$, where $b_1, b_2 > 0$. The problem of density estimation in our case is to approximate the resulting joint distribution $p(\mathbf{x})$. Since we wish to generate new samples, our problem is to optimize the set of parameters ψ for the mapping $M : \mathbf{x} \xrightarrow{p(\mathbf{x};\psi)} \tilde{\mathbf{x}}$, where $\tilde{\mathbf{x}}$ is a fake but realistic synthetic auction, i.e., it is impossible to say if $\tilde{\mathbf{x}} \sim p(\mathbf{x})$ or $\tilde{\mathbf{x}} \sim p(\cdot)$, where $p(\cdot)$ is an arbitrary probability function.

By breaking down the mapping M into two independent and sequential ones, namely by considering the functions $A : \mathbf{z} \xrightarrow{p(\mathbf{c}|\mathbf{z};\alpha)} \tilde{\mathbf{c}}$ and $B : \mathbf{c} \xrightarrow{p(\mathbf{b}|\mathbf{c};\beta)} \hat{\theta}$, we can alleviate the technical difficulties exposed in Section 3. The function A produces fake samples of auction characteristics $\tilde{\mathbf{c}}$ from the noise input \mathbf{z} , by approximating $p(\mathbf{c}|\mathbf{z};\alpha)$ using the set of parameters α . It is convenient to rely on the latent signal \mathbf{z} because fake samples can be generated from scratch, the real data being needed only for the training of such approximator. The function B approximates the conditional distributions of the bids given auction features, and therefore provides an aggregated representation of the firms. The vector $\hat{\theta}$ is composed of the estimated parameters to the conditionals, and depends on the probability function used to describe the distribution of bids. The bid generator B hence generates estimates that, in turn, serve as arguments to a random generator from which nb bids are sampled, i.e., $\hat{\mathbf{b}} \sim \mathcal{P}(\hat{\theta})$.

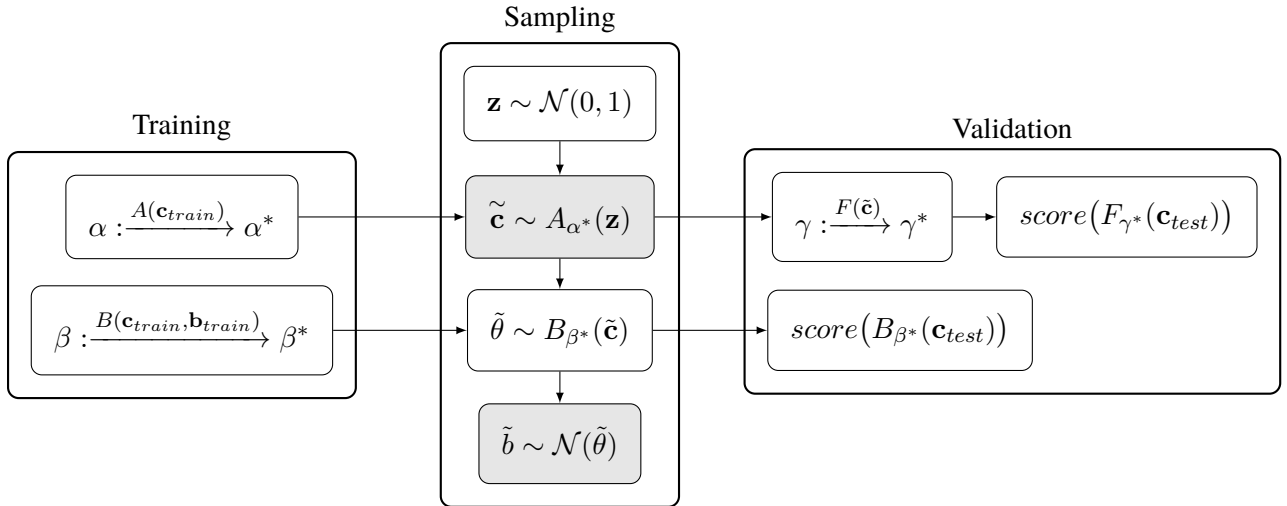
No functional forms have been chosen for A and B yet, but we can already see the general structure conveniently articulates. Indeed, once both models are trained (w.r.t α and β), we can sample fake but realistic vectors of auction features $\tilde{\mathbf{c}}$ using A , that are in turn used as input for B , reconstructing the space $\{\mathbf{c}, \mathbf{b}\}$. Thereby, the generation of each data type is separated between A (discrete) and B (continuous), and the multi-level auction structure is now flattened since B represents all the firms at once. At this stage, the

problem previously formalized by the mapping M , has been divided into A and B , or equivalently, we just defined $\psi = (\alpha, \beta)$.

This pipeline does not explicitly include the multi-label variable $firms$, whose cardinality is too big to even try to preserve its original form and interpretability. In addition, we fail to see the point of using a smaller continuous code representing $firms$, if it is not possible to retrieve the original space afterwards. It should also be noted that keeping only a subset of the data in order to lower the cardinality would defeat the purpose. Nevertheless, later in Section 6, we discuss a solution that allows an explicit representation of the bidders when their number is manageable.

Finally, the validation follows the inception scoring method, by training a predictor F with the synthetic data newly sampled, and by evaluating its performances on the real data. The bid generator is then evaluated separately with real examples unseen during training. Figure 4.1 provides a visual map of the overall system we just described.

Figure 4.1: Graph showing the sequential structure of our meta-algorithm. The training phase involves the optimization of α and β using a training set composed of real examples. The sampling phase uses the trained functions A^* and B^* in order to generate $D_{synth} = \{\tilde{\mathbf{c}}, \tilde{\mathbf{b}}\}$ (nodes in grey).



4.1 Generating Synthetic Auction Features

Following the layout proposed by Figure 4.1, here we linger on the specification, and the details regarding the training, of two deep generative models respectively based on GANs and VAEs, chosen to perform the task $A : \mathbf{z} \xrightarrow{p(\mathbf{c}|\mathbf{z};\alpha)} \tilde{\mathbf{c}}$. It is important to understand that those two models are not complementary, but are competitors. It is a priori not possible to foresee which one would perform the best, so we have decided to try them both.

4.1.1 GAN-based Approach

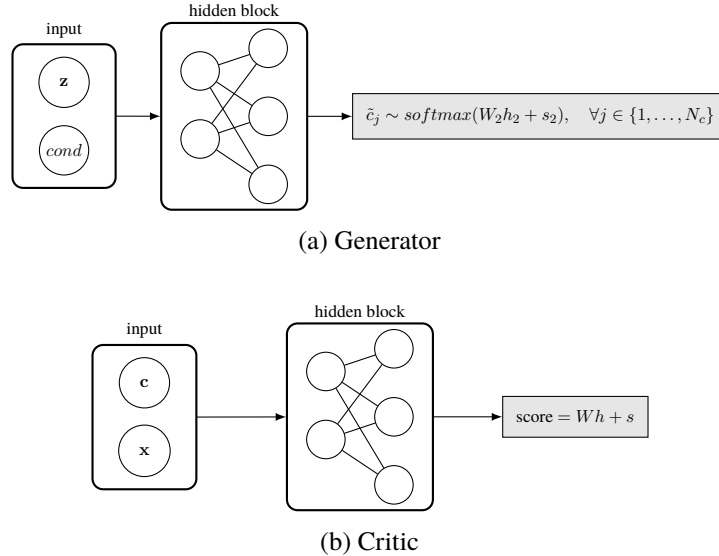
Following the literature presented in Section 3, our GAN-based algorithm articulates around a generator G and a critic C , that are to be optimized with respect to the Wasserstein loss. We also include our model in a *training-by-sampling* framework, meaning that G now approximates $p(\mathbf{c}|\mathbf{z}, cond)$, where $cond$ is a binary conditional vector of size $|C|$ that sums to one. To that end, our loss function needs to be augmented with a

cross-entropy penalty term that enforces the sampling of a synthetic data point admitting $c_{i^*} = 1$, where i^* is the selected state of the selected variable c . The resulting objective function writes as

$$\min_G \max_C E \left[C(G(\mathbf{z})) - C(\mathbf{c}) \right] + CE(\tilde{c}_{i^*}, cond). \quad (3)$$

The training procedure that revolves around Equation (3) is detailed by Algorithm 1, while Figure 4.2 makes a graphical account for the algorithmic architecture of the GAN-based model used in this study. We have followed the PacGAN configuration [37] by expanding the critic’s input space with 10 stacks of the original space to prevent mode collapse [36], and we have applied a penalty to the norm of the critic’s gradient with respect to its input to achieve a faster and more stable learning. Gradient penalty (WGAN-GP) is used in replacement to *weight clipping*, which consists in imposing a Lipschitz constraint on the critic [43]. Another important point is, as explained in Section 2, the discriminator and the generator need to be optimized in a synchronized way in the vanilla GANs framework. In Wasserstein optimization, however, it seems that the generator needs to be optimized as many times as the critic, which tends to dominate the generator very quickly otherwise. An extension of the *stochastic gradient descent* called *Adam* was used as optimizer as it is customary. The latter improves performances by maintaining an adaptive learning rate that evolves in regard to the context.

Figure 4.2: Neural representation of the generator and the critic used to synthesize auction characteristics. Note that W and s are respectively weight matrices and biases, while h are outputs from hidden blocks. The dimensions of h , and therefore of W and s , depend on the width parameters for a given network. The critic C outputs a scalar while G outputs a continuous array of size N_x (the number of continuous variables) and N_c onehot arrays (one for each discrete multi-class variable).



4.1.2 Tabular Variational Autoencoding

VAEs are good alternatives to GANs, and are relatively easy to accommodate for tabular data. Indeed, the reconstruction loss is based on the KL divergence between two continuous signals (see Equation (2)), and is thus more robust to differentiability issues. Another key difference is that the decoder receives an explicit signal from the loss function during training, while the generator in GANs only learns through the discriminator or the critic, as shown by Figure 2.2. Consequently, only the decoder needs to be modified to generate tabular data using variational autoencoding. The encoder models $p(\mathbf{z}|\mathbf{c}, \mathbf{x})$, while the decoder replicates the original

Algorithm 1 Training GANs-based auction features generator

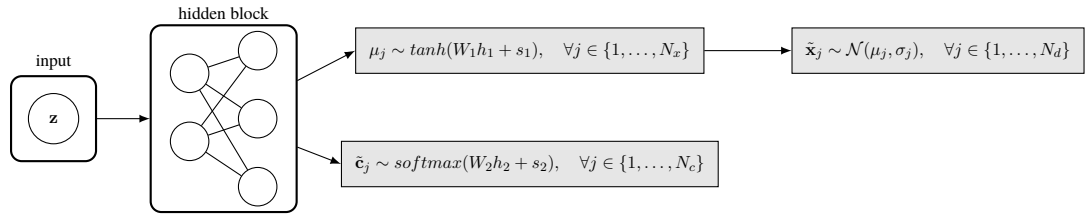
```

1:  $D_{train} \leftarrow$  Initialize training set
2: while  $C(fake) > threshold$  do ▷ The critic can be optimized until  $C(fake)$  is near 0.
3:   Randomly select a discrete variable  $c$  with equal probability
4:   Compute the probability mass function (PMF) of  $c$ 
5:   Randomly select a state  $i^*$  inherent to  $c$  according its PMF
6:   Create the conditional vector  $cond$  so that  $\sum_i cond(i) = 1$  and  $cond(i^*) = 1$ 
7:   for  $batch \in \{1, \dots, N_{batches}\}$  do ▷ Gradient descent with mini-batch
8:      $real \leftarrow d(c_{i^*} = 1) \sim D_{train}$  ▷ Sample batch of real examples respecting the constraint
9:      $z \sim \mathcal{N}(0, 1)$  ▷ Sample noise
10:     $fake \leftarrow \tilde{d} \sim G(z)$  ▷ Sample fake examples
11:     $real \leftarrow [real] \times 10$  ▷ Stack input 10 times for Pac configuration
12:     $fake \leftarrow [fake] \times 10$ 
13:     $L^j \leftarrow (C(fake_j) - C(real_j)) + CE(\tilde{c}, cond)$ 
14:     $L^{batch} \leftarrow L^{batch} + \lambda(\|\nabla L^{batch}\|_2 - 1)^2$  ▷ Apply gradient penalty
15:     $w_{crit} \leftarrow w_{crit} + Adam(\nabla_{w_{crit}} \frac{1}{m} \sum_i L^{batch}(i))$  ▷ Updating  $C$  with Adam
16:    if  $batch \bmod k = 0$  then ▷ Synchronicity, depends on  $k$ 
17:       $w_{gen} \leftarrow w_{gen} + Adam(\nabla_{w_{gen}} \frac{1}{m} \sum_i -C(G(z)))$  ▷ Updating  $G$  with Adam

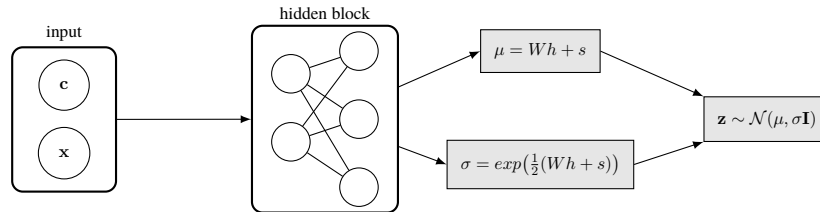
```

space by approximating $p(\mathbf{c}, \mathbf{x}|\mathbf{z})$. *Training-by-sampling* has no equivalent in the VAEs framework since the conditional vector would be encoded in a continuous layer, making the use of VAEs for discrete data more straightforward. The neural representation of the tabular VAE is given by Figure 4.3, and Algorithm 2 gives the specific steps to its training. Note that the encoder and decoder are updated simultaneously, meaning that from a training perspective they share the same set of parameters. Although *training-by-sampling* is not applicable here, the reconstruction loss still needs to be augmented with a cross-entropy term to ensure the integrity of the discrete structure.

Figure 4.3: Neural representation of the encoder and decoder composing the tabular VAE used to synthesize auction characteristics. Similarly to Figure 4.2, W and s are respectively weight matrices and biases, while h are outputs from hidden blocks. The σ_j are parameters to the decoder.



(a) Decoder



(b) Encoder

Algorithm 2 Training tabular VAE for auction features

```

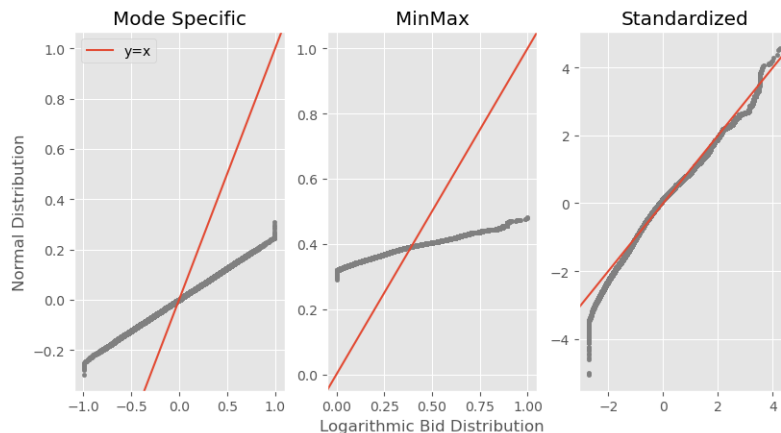
1:  $D_{train} \leftarrow$  Initialize training set
2: for  $epoch \in N_{steps}$  do
3:   for  $batch \in \{1, \dots, N_{batches}\}$  do ▷ Gradient descent with mini-batch
4:      $real \sim D_{train}$  ▷ Sample batch of real examples
5:      $(\mu, \sigma^2) \sim Enc(real)$ 
6:      $z \sim \mathcal{N}(\mu, \sigma^2)$  ▷ Sample latent input
7:      $fake \sim Dec(z)$  ▷ Sample fake examples
8:      $L^j \leftarrow CE(\tilde{c}_j - \arg \max(c)) + (2\sigma^2)^{-1}(x_j - \tanh(\tilde{x}_j))^2 + KL(\mathcal{N}(\mu_j, \sigma_j^2), \mathcal{N}(0, 1))$ 
9:      $w \leftarrow w + Adam(\nabla_w \frac{1}{m} \sum_i L^{batch}(i))$  ▷ Updating parameters with Adam

```

4.2 Training a Generator of Continuous Bids

We recall that B must represent all the firms at once by learning a bidding function based on auction features, which are synthesized with A . At the end, we plan to choose the best out of the two models trained for A , but for now this information is irrelevant, since we only need to consider inputs sampled from the original data in order to train an approximator $B : \mathbf{c} \xrightarrow{p(b|\mathbf{c};\beta)} \hat{\theta}$. As shown by Figure 4.4, the standardized logarithmic bid distribution is Gaussian, and accordingly, we can make the assumption of log-normality for the conditionals, meaning that $\theta = (\mu, \sigma^2)$ where μ and σ^2 are the first two moments of the Gaussian density. According

Figure 4.4: Comparison of normal quantile-to-quantile plots relating to several numerical representations of the logarithmic bids. Left to right: mode specific normalization, minmax normalization and standardization. Here, mode specific normalization was applied on the bids in hope that it would provide a finicky representation of the target, in regard to the incumbent regression task.



to the pipeline described earlier, the input space of the bid generator B must match the output space of the auction generator A . The challenge here arises from the fact that the bids must be generated separately, but not independently from their conditional vector. Since θ is a bi-dimensional vector, the task at hand is defined as a multi-output regression. A multi-output linear model being merely the fit of independent models, since the statistical dependence between each model's set of parameter is ignored, a nonlinear approximator is required in order to model B .

A neural network is the most general approximator being able to perform multi-target regression, while preserving the statistical dependence among its parameters [3]. Furthermore, considering an input vector x and a target y a NN, or *multi-layer perceptron* (MLP), can represent the function $f(x; \gamma)$ by producing

the parameters for a distribution over y rather than a direct prediction of y [47, 48, 49]. This applies when γ is optimized with respect to $-\log P(y|x)$. Considering a MLP for A , we understand its output as a bi-dimensional vector containing the predicted first two moments of a conditional distribution $p(b|c)$. We will refer to such model as the *BidNet*.

In order to make sure of its stability (i.e., systematic convergence), we trained the BidNet on different folds, using a *cross-validation* procedure. The idea is to divide the training set into K folds ($K = 5$ in our case), and to use $K - 1$ folds to optimize the parameters with respect to the *negative log-likelihood* (NLL), and then to compute the aggregated loss on the remaining fold. The validation set (the remaining fold) is used after each pass over the training set in order to assess the objective NLL upon which an *early stopping* rule is based. This strategy counts as a regularization method to avoid overfitting. This process is repeated until the K folds have served as validation set. Although several early-stopping designs have been identified by [50], we used a customized one that fits best our needs. The pseudo-code inherent to the training of the BidNet with cross-validation is given in Algorithm 3.

Algorithm 3 K-folds cross-validation BidNet training procedure

```

1:  $D \leftarrow \{D_1, \dots, D_K\}$  ▷ Initialize K-folds
2:  $loss^* \leftarrow \infty$  ▷ Initialize best model
3: for  $fold \in D$  do
4:    $reset(w_{BidNet})$  ▷ Reset parameters before entering each new fold
5:    $D_{val} \leftarrow D(fold), D_{train} \leftarrow D(-fold)$ 
6:   while has not converged do
7:     for  $batch \in \{1, \dots, N_{batches}\}$  do ▷ Gradient descent with mini-batch
8:        $d \sim D_{train}$  ▷ Sample batch of real examples
9:        $\hat{\theta} \leftarrow BidNet(d)$ 
10:       $L^{train} \leftarrow m^{-1} \sum_i NLL(\hat{\theta})_i$  ▷ compute NLL on training batch
11:       $w \leftarrow w + Adam(\nabla L^{train})$  ▷ Update BidNet
12:       $converged \leftarrow ES(L^{val})$  ▷ Early stopping
13:       $L^{val} \leftarrow n^{-1} \sum_j NLL(BidNet(D_{val}))_j$  ▷ compute NLL on validation fold
14:      if  $L^{val} < loss^*$  then
15:         $loss^* \leftarrow L^{val}$ 
16:        save model

```

4.3 Sampling Synthetic Public Procurement Instances

The GAN-based model relies on its generator to sample synthetic features from a noise. However, following the principle of training-by-sampling, the user must also create a conditional vector, or a batch of conditional vectors, alongside the latent space \mathbf{z} . To that end, one must apply the steps 3 to 6 described in Algorithm 1, and then feed the trained generator with the noise and the conditional vector, as shown in Figure 4.2. The advantage here is that one can manually specify a conditional vector—by ignoring steps 3 to 5 in Algorithm 1—in order to replicate the signal of interest. The tabular VAE also samples through a latent noise that can be created from a standard Gaussian distribution.

A synthetic instance of public procurement is then the concatenation of a vector of auction features $\tilde{\mathbf{c}}$ and of its associated array of bids. We recall that the process of bid generation unfolds in two steps because the number of bids to be generated per auction varies. The variable *number of bidders* encodes this information and has been included in the joint distribution of auction characteristics, and therefore is included in the output of A . Since the BidNet predicts the first moments of a Gaussian distribution, it is straightforward to

sample nb bids from a random generator. Indeed, when given synthetic inputs coming from A , the BidNet provides $\tilde{\theta} = (\tilde{\mu}, \tilde{\sigma}^2)$, the parameters to the conditionals $p(b|\mathbf{c}; \theta)$. Then, synthetic bids are drawn according to $\tilde{b} \sim \mathcal{N}(\tilde{\theta})$. To be consistent with the notation introduced in Figure 4.1, we distinguish \tilde{b} from \hat{b} , the latter being the predicted bids emanating from $\mathcal{N}(\hat{\theta})$, where $\hat{\theta}$ is the output of the BidNet when given an original sample from the test set \mathbf{c}_{test} . Note that the predicted bids \hat{b} are to be used for validation purposes only.

5 Validation

To begin with, we assess the faithfulness of the synthetic auction features, and by extension the performances of our synthesizers, with an inception score. We recall that the goal of a synthesizer is to generate fresh samples that are not seen in the original data, but that presumably emanate from the same generative process. Sometimes, one may even require from a synthesizer to sample exclusively new examples, as it is the case when privacy is a concern, but this topic is beyond the scope of this study. An inception score is based on the principle that the properties of a predictor’s output are function of the input, given a fixed set of parameters. Therefore, a regressor or a classifier successfully trained using synthetic data is expected to display a satisfying performance on a test-bed composed of real instances. A good description of such procedure is, among others, available in [46]. In our case, we use the binary variable *municipality*—one of the auction characteristics—as a target in the following binary classification problem:

$$f(\mathbf{c}_{-mun}) = p(mun),$$

where \mathbf{c}_{-mun} is the onehot encoded set of auction features that excludes *municipality*. In other terms, we define the classifier $f : \frac{p(mun|\mathbf{c}_{-mun})}{p(mun|\mathbf{c}_{-mun})} \rightarrow [0, 1]$. If the synthetic data is realistic, that is, if the synthesizer being evaluated managed to efficiently approximate the targeted joint distribution, then we expect the overall accuracy to $f(\mathbf{c}_{-mun})$ and $f(\tilde{\mathbf{c}}_{-mun})$ to be similar; providing f has been successfully trained.

Three models were used to represent the classifier f : a *decision tree*, *k-nearest neighbors* (k-NN) and a *multi-layer perceptron* (MLP). Table 2 reports evaluation metrics for the three classifiers when trained on synthetic examples generated by the GAN-based (Table 2 (a)) and VAE-based (Table 2(b)) methods. Based on the results reported in Table 2, we can draw a straightforward conclusion: the GAN-based model succeeded to synthesize reliable and realistic data, but the VAE-based model did not. Indeed, the neural network (MLP) achieved an overall classification F1-score on the real test-bed of only 1% below what was achieved on the synthetic test-bed. We recall that, having been trained with synthetic data, it is natural that the classifiers perform best on an synthetic test-bed. Even if the decision tree model performed the worst with a F1-score 15% below its reference point, it has still achieved a 78%, which is acceptable according to classification standards. Furthermore, we can see that a specific pattern emerges from this experiment, namely, it seems that instances belonging to class 0 are more accurately classified than those of class 1 (Recall (0) versus Recall (1)). All three classifiers have preserved this structure when tested with real data; another evidence supporting our conclusion. When looking at Table 2 (b), however, classifiers display relatively bad F1-score, ranging from 44% (Decision Tree) to 75% (MLP). A F1-score below or around 50% indicates that the classifier was not better than a random algorithm. In addition, the decision tree and the k-NN both assigned all instances of the real test-bed to the same class (class 0 for the decision tree and class 1 for the k-NN). The MLP did some decent work in recognizing some structure in the data generated by the VAE-based model, but the scores achieved on the synthetic test-bed are unrealistically high. This gap in performance between the GAN and VAE-based methods explains why we indulged in the specification of two methods in the first place. It should also be noted that the results in this kind of experiment may vary according to the hyperparameter settings, and in theory, the tabular VAE should be able to reach a similar level of effectiveness with some fine tuning.

Table 2: The classification accuracy for each class (Recall), as well as the average F1-score are reported. The classifiers have been trained two times each, using 100,000 training examples generated with the GANs and VAE-based method. Both synthesizers have been previously trained over 200 epochs. The numbers in the parenthesis indicate the performance gap (in percentage) between scores achieved on synthetic and real test-beds.

(a) Evaluation metrics of models trained on synthetic data generated by the GAN-based method.

Test-bed	Model	Recall (0)	Recall (1)	F1-score
Synthetic	Decision Tree	0.95	0.91	0.93
	k-NN	0.90	0.84	0.87
	MLP	0.88	0.80	0.84
Real	Decision Tree	0.94 (-0.01)	0.57 (-0.15)	0.78 (-0.15)
	k-NN	0.81 (-0.09)	0.74 (-0.10)	0.78 (-0.09)
	MLP	0.88 (0.00)	0.76 (-0.04)	0.83 (-0.01)

(b) Evaluation metrics of models trained on synthetic data generated by the VAE-based method.

Test-bed	Model	Recall (0)	Recall (1)	F1-score
Synthetic	Decision Tree	0.99	1.00	0.99
	k-NN	0.98	0.96	0.97
	MLP	0.98	0.97	0.97
Real	Decision Tree	1.00 (+0.01)	0.00 (-1.00)	0.44 (-0.55)
	k-NN	0.00 (-0.98)	1.00 (+0.04)	0.24 (-0.73)
	MLP	0.66 (-0.32)	0.89 (-0.08)	0.75 (-0.22)

The point to be made here, is that the GAN-based model provides a reliable way to perform the task at hand without having to worry too much about hyperparameter tuning.

Now we need to evaluate the efficiency of the BidNet, and by extension the reliability the synthetic bids. An account of the BidNet’s relative efficiency is given by Table 3. The BidNet was compared to a *regression tree* model and a *multi-target support vector regressor* (MSVR). The three regressors have been evaluated using the same metric—negative log-likelihood (NLL)—and Table 2 reports their performances over five folds. The BidNet is in average the best model, and also the faster.

Table 3: The averages and standard deviations of the negative log-likelihood (NLL) over the five cross-validation folds are given for the BidNet, a tree-based regressor and a multi-target support vector regressor (MSVR). The column *best* reports the NLL to the best model identified with each method.

Model	NLL			Number of Iteration	
	mean	std	best	mean	std
BidNet	0.81	0.61	0.10	1,184	6,445
Regression Tree	2.11	0.03	2.06	92,500	-
MSVR	1.61	0.07	1.50	92,500	-

Nevertheless, since the NLL is a relative measure with values that can range from $-\infty$ and $+\infty$, a thorough investigation of the BidNet’s outputs is needed in order to assert the reliability of the resulting synthetic bid distribution. To that end, we propose the procedure detailed in Algorithm 4.

The idea is to evaluate the distance between the distributions of fake and real bids, $Dist(p(b)||p(\tilde{b}))$, using the distance between the real and predicted distributions $Dist(p(b)||p(\hat{b}))$ as an identity, and the distance

Algorithm 4 Synthetic bid validation / Double validation

- 1: $\beta \leftarrow \beta^*$ ▷ load best set of parameters for BidNet
 - 2: $\alpha \leftarrow \alpha^*$ ▷ load optimized set of parameters for synthesizer
 - 3: $\tilde{\mathbf{c}} \sim A_{\alpha^*}(\mathbf{z})$ ▷ sample synthetic examples from the trained synthesizer
 - 4: $\mathbf{c} \sim D_{test}$ ▷ sample a test-set of real instances
 - 5: $\hat{b} \sim B_{\beta^*}(\mathbf{c})$ ▷ sample predicted bids from the test-set of real instances using the BidNet
 - 6: $\tilde{b} \sim B_{\beta^*}(\tilde{\mathbf{c}})$ ▷ sample fake bids with the synthetic data emanating from the synthesizer
 - 7: $Dist(p(b)||p(\tilde{b}))$ ▷ compute the statistical distance between the fake and real distributions of bids
 - 8: $Dist(p(b)||p(\hat{b}))$ ▷ compute the statistical distance between the predicted and real distributions of bids
 - 9: $Dist(p(\hat{b})||p(\tilde{b}))$ ▷ compute the statistical distance between the predicted and fake distributions of bids
-

between the predicted and fake distributions $Dist(p(\hat{b})||p(\tilde{b}))$ as a control. Algorithm 4 is also coined “double validation” because it provides another way to validate the output of the synthesizers. Indeed, the opportunity to use the BidNet in order to construct an inception score naturally occurs since it has been trained on the real data, and generates synthetic bids from fake auction features. Table 4 reports results coherent with those of Table 2 as the tabular VAE is at the origin of a noisy synthetic bid distribution, meanwhile $Dist(p(b)||p(\tilde{b}))$ and $Dist(p(\hat{b})||p(\tilde{b}))$ are very close of each other in both cases, and also close to $Dist(p(b)||p(\hat{b}))$ in the GAN-generated data case. The BidNet is hence effective in preserving the statistical dependence between bids and their auction features, and is a powerful approximator of $p(b|\mathbf{c})$.

Table 4: The statistical distances have been measured with the *Wasserstein* or *Earth-Mover Distance* (EMD), and the *quantile-to-quantile root mean squared error* (QQ-RMSE). A score of 0 indicates identical distributions.

(a) Synthetic bids emanate from the real data.

	QQ-RMSE	EMD
$Dist(p(b) p(\hat{b}))$	1.17	0.02

(b) Synthetic bids emanate from the data generated by the GAN-based method.

	QQ-RMSE	EMD
$Dist(p(b) p(\tilde{b}))$	1.37	0.01
$Dist(p(\hat{b}) p(\tilde{b}))$	1.30	0.00

(c) Synthetic bids emanate from the data generated by the VAE-based method.

	QQ-RMSE	EMD
$Dist(p(b) p(\tilde{b}))$	400.55	0.28
$Dist(p(\hat{b}) p(\tilde{b}))$	400.55	0.30

6 Discussion

In this paper, we have tackled the problem of density approximation with discrete deep learning and deep generative models for the sampling of artificial instances of public procurement data. Because of the excessive cardinality and combinatorial nature of the bidder space, our sampling system includes two sequential compartments: a generator of auction features and a generator of bids. The bid generator (BidNet) is a

MLP trained to predict the parameters of the conditional bid distributions from auction features. We also have trained two models, based on the two most powerful algorithmic classes (GANs and VAEs) of deep synthesizers, on the task to approximate and sample from the joint distribution of auction features. Finally, we have shown the efficacy of our generative system with a validation procedure that includes a state-of-the-art inception scoring method, that we have cross-validated with a supplementary step that takes advantage of the specific structure of our system.

Alternatively, if the multi-label space is of reasonable size, it is possible to generate fake public procurement instances that include an explicit representation of the bidding firms. To that end, a multi-label predictor of binary values must be optimized simultaneously within a GANs structure. This is the idea adopted by the MEDGAN ([9]), which uses an autoencoder in order to reconstruct the multi-label space in the same time that the rest of the joint distribution is being replicated. The MEDGAN has been originally developed for medical records, providing a way to deal with the multi-label structure of patient characteristics.

Even though the tabular VAE is in theory a reliable method, the conditional tabular GANs framework is in general superior, because it allows the practitioner to generate synthetic data based on a conditional vector that can be specified manually. Data amplification and balancing can hence be targeted, and the generation of synthetic data can be focused on a particular conditional space. The two examples that come naturally in mind from the standpoint of economics research are: counterfactual analysis and simulation-based modeling.

Deep generative models are useful by providing the statistical balance necessary to conduct counterfactual analysis with distance metrics such as propensity scores. In addition, DGMs can directly be used in order to sample counterfactual instances. In other words, DGMs carry the potential of being genuine assets in the search of causal effects. We also argued that the deep generative techniques can potentially invigorate research designs such as agent-based modeling by providing an pseudo-unlimited stream of realistic data, upon which artificial agents can be trained to reproduce or predict socio-economic behaviors. For example, in the case of public procurement, we can envision a DGM-powered simulation or environment in which artificial agents could represent firms or public organisms. More generally, economic questions could be more easily studied from the lens of agent-based modeling, in a game-theoretic fashion, thanks to the support of computational experiments made possible by powerful data generators.

Acknowledgements

The authors are grateful to Meta Research for their financial support granted following the authors application to the request for proposals on [agent-based user interaction simulation to find and fix integrity and privacy issues](#).

Declarations of Interest

The authors declare no competing interests.

References

- [1] S. Athey, “The Impact of Machine Learning on Economics,” *The Economics of Artificial Intelligence: An Agenda* (2019) 507–552. <https://doi.org/10.7208/9780226613475-023>.
- [2] S. Mullainathan and J. Spiess, “Machine learning: An applied econometric approach,” *Journal of Economic Perspectives* **31** no. 2, (2017) 87–106.

- [3] I. Goodfellow, Y. Bengio, and A. Courville, *Deep Learning*. The MIT Press, 2016.
- [4] D. P. Kingma and M. Welling, “Auto-encoding variational bayes,” in *2nd International Conference on Learning Representations, ICLR 2014 - Conference Track Proceedings*, no. M1, pp. 1–14. 2014. [arXiv:1312.6114](https://arxiv.org/abs/1312.6114).
- [5] S. Athey and G. W. Imbens, “Machine Learning Methods That Economists Should Know About,” *Annual Review of Economics* **11** no. 1, (2019) 685–725, [arXiv:1903.10075](https://arxiv.org/abs/1903.10075). <https://www.gsb.stanford.edu/faculty-research/working-papers/machine-learning-methods-economists-should-know-about>.
- [6] M. Lucic, K. Kurach, M. Michalski, O. Bousquet, and S. Gelly, “Are Gans created equal? A large-scale study,” *Advances in Neural Information Processing Systems* **2018-Decem** no. Nips, (2018) 700–709, [arXiv:1711.10337](https://arxiv.org/abs/1711.10337).
- [7] V. Borisov, T. Leemann, K. Seßler, J. Haug, M. Pawelczyk, and G. Kasneci, “Deep Neural Networks and Tabular Data: A Survey,” [arXiv:2110.01889](https://arxiv.org/abs/2110.01889). <http://arxiv.org/abs/2110.01889>.
- [8] H. Ba, “Improving Detection of Credit Card Fraudulent Transactions using Generative Adversarial Networks,” [arXiv:1907.03355](https://arxiv.org/abs/1907.03355). <http://arxiv.org/abs/1907.03355>.
- [9] P. Jackson and M. Lussetti, “Extending a Generative Adversarial Network to Produce Medical Records with Demographic Characteristics and Health System Use,” *2019 IEEE 10th Annual Information Technology, Electronics and Mobile Communication Conference, IEMCON 2019* (2019) 515–518.
- [10] Z. Cai, Z. Xiong, H. Xu, P. Wang, W. Li, and Y. Pan, “Generative Adversarial Networks: A Survey Toward Private and Secure Applications,” *ACM Computing Surveys* **54** no. 6, (2021) , [arXiv:2106.03785](https://arxiv.org/abs/2106.03785).
- [11] J. Yoon, J. Jordon, and M. Van Der Schaar, “Ganite: Estimation of individualized treatment effects using generative adversarial nets,” *6th International Conference on Learning Representations, ICLR 2018 - Conference Track Proceedings* no. 2010, (2018) 1–15. <https://openreview.net/pdf?id=ByKWUeWA->.
- [12] C. Louizos, U. Shalit, J. Mooij, D. Sontag, R. Zemel, and M. Welling, “Causal effect inference with deep latent-variable models,” *Advances in Neural Information Processing Systems* **2017-Decem** no. Nips, (May, 2017) 6447–6457, [arXiv:1705.08821](https://arxiv.org/abs/1705.08821). <http://arxiv.org/abs/1705.08821>.
- [13] R. Cai, J. Qiao, K. Zhang, Z. Zhang, and Z. Hao, “Causal discovery with cascade nonlinear additive noise models,” *IJCAI International Joint Conference on Artificial Intelligence* **2019-Augus** (2019) 1609–1615, [arXiv:1905.09442](https://arxiv.org/abs/1905.09442).
- [14] B. W. Arthur, S. N. Durlauf, and D. A. Lane, eds., *The Economy as an Evolving Complex System II*. Perseus Books Publishing, a procedi ed., 1997.
- [15] L. Tesfatsion, “Agent-Based Computational Economics: Modelling Economies as Complex Adaptive Systems,” in *Proceedings of the Joint Conference on Information Sciences*, vol. 6, pp. 40–43. 2002. <http://www.econ.iastate.edu/tesfatsi/>.
- [16] J. Angrist, P. Azoulay, G. Ellison, R. Hill, and S. F. Lu, “Economic research evolves: Fields and styles,” *American Economic Review* **107** no. 5, (2017) 293–297.
- [17] R. L. Axtell and J. D. Farmer, “Agent-Based Modeling in Economics and Finance: Past, Present, and Future,” *Journal of Economic Literature* no. August 2018, (2021) to appear.

- [18] M. Wong and B. Farooq, “A bi-partite generative model framework for analyzing and simulating large scale multiple discrete-continuous travel behaviour data,” *Transportation Research Part C: Emerging Technologies* **110** (Jan, 2020) 247–268, [arXiv:1901.06415](https://arxiv.org/abs/1901.06415).
- [19] R. Salakhutdinov and G. Hinton, “Deep Boltzmann machines,” *Journal of Machine Learning Research* **5** no. 3, (2009) 448–455.
- [20] G. Marti, “CORRGAN: Sampling Realistic Financial Correlation Matrices Using Generative Adversarial Networks,” in *ICASSP 2020 - 2020 IEEE International Conference on Acoustics, Speech and Signal Processing (ICASSP)*, pp. 8459–8463. Oct, 2020. [arXiv:1910.09504](https://arxiv.org/abs/1910.09504). <http://arxiv.org/abs/1910.09504>.
- [21] S. Takahashi, Y. Chen, and K. Tanaka-Ishii, “Modeling financial time-series with generative adversarial networks,” *Physica A: Statistical Mechanics and its Applications* **527** (Aug, 2019) .
- [22] M. Dotoli, N. Epicoco, and M. Falagario, “Multi-Criteria Decision Making techniques for the management of public procurement tenders: A case study,” *Applied Soft Computing Journal* **88** (Mar, 2020) .
- [23] E. J. Green and R. H. Porter, “Noncooperative Collusion under Imperfect Price Information,” *Econometrica* **52** no. 1, (1984) 87.
- [24] Y. Chassin and M. Joanis, “Détecter et prévenir la collusion dans les marchés publics en construction: Meilleures pratiques favorisant la concurrence,” 2010. <https://www.researchgate.net/publication/254398401> { % } 0AD { é } tecter.
- [25] A. Skrzypacz and H. Hopenhayn, “Tacit collusion in repeated auctions,” *Journal of Economic Theory* **114** no. 1, (Jan, 2004) 153–169.
- [26] J. Miklós-Thal and C. Tucker, “Collusion by algorithm: Does better demand prediction facilitate coordination between sellers?,” *Management Science* **65** no. 4, (Apr, 2019) 1552–1561.
- [27] S. O. Kimbrough, M. Lu, and F. Murphy, “Learning and Tacit Collusion by Artificial Agents in Cournot Duopoly Games,” in *Formal Modelling in Electronic Commerce*, pp. 477–492. Springer-Verlag, Dec, 2005.
- [28] A. Itto and N. Petit, “Algorithmic Pricing Agents and Tacit Collusion: A Technological Perspective,” *SSRN Electronic Journal* (Oct, 2017) .
- [29] U. Schwalbe, “Algorithms, Machine Learning, and Collusion,” *Journal of Competition Law & Economics* **14** no. 4, (Dec, 2018) 568–607.
- [30] A. C. Tellidou and A. G. Bakirtzis, “Agent-based analysis of capacity withholding and tacit collusion in electricity markets,” *IEEE Transactions on Power Systems* **22** no. 4, (Nov, 2007) 1735–1742.
- [31] N. Rashedi, M. A. Tajeddini, and H. Kebriaei, “Markov game approach for multi-agent competitive bidding strategies in electricity market,” *IET Generation, Transmission and Distribution* **10** no. 15, (2016) 3756–3763. <https://www.researchgate.net/publication/305627052>.
- [32] Y. Ye, D. Qiu, M. Sun, D. Papadaskalopoulos, and G. Strbac, “Deep Reinforcement Learning for Strategic Bidding in Electricity Markets,” *IEEE Transactions on Smart Grid* (Aug, 2019) 1–1.
- [33] M. Shafie-Khah and J. P. Catalão, “A stochastic multi-layer agent-based model to study electricity market participants behavior,” *IEEE Transactions on Power Systems* **30** no. 2, (Mar, 2015) 867–881.

- [34] Z. Zhou, W. K. Chan, and J. H. Chow, “Agent-based simulation of electricity markets: A survey of tools,” *Artificial Intelligence Review* **28** no. 4, (Dec, 2007) 305–342.
- [35] H. Larochelle and I. Murray, “The Neural Autoregressive Distribution Estimator,” in *Proceedings of the Fourteenth International Conference on Artificial Intelligence and Statistics*, G. Gordon, D. Dunson, and M. Dudík, eds., vol. 15 of *Proceedings of Machine Learning Research*, pp. 29–37. PMLR, Fort Lauderdale, FL, USA, 2011. <https://proceedings.mlr.press/v15/larochelle11a.html>.
- [36] T. Salimans, I. Goodfellow, W. Zaremba, V. Cheung, A. Radford, X. Chen, and X. Chen, “Improved Techniques for Training GANs,” in *Advances in Neural Information Processing Systems*, D. Lee, M. Sugiyama, U. Luxburg, I. Guyon, and R. Garnett, eds., vol. 29, pp. 1–9. Curran Associates, Inc., Dec, 2016. [arXiv:1701.00160](https://arxiv.org/abs/1701.00160). <http://arxiv.org/abs/1701.00160https://proceedings.neurips.cc/paper/2016/file/8a3363abe792db2d8761d6403605aeb7-Paper.pdf>.
- [37] Z. Lin, G. Fanti, A. Khetan, and S. Oh, “PacGan: The power of two samples in generative adversarial networks,” *Advances in Neural Information Processing Systems 2018-December* no. 8, (2018) 1498–1507, [arXiv:1712.04086](https://arxiv.org/abs/1712.04086).
- [38] D. M. Blei, A. Kucukelbir, and J. D. McAuliffe, “Variational Inference: A Review for Statisticians,” *Journal of the American Statistical Association* **112** no. 518, (Jan, 2017) 859–877, [arXiv:1601.00670](https://arxiv.org/abs/1601.00670). <http://arxiv.org/abs/1601.00670http://dx.doi.org/10.1080/01621459.2017.1285773https://doi.org/10.1080/01621459.2017.1285773>.
- [39] C. Doersch, “Tutorial on Variational Autoencoders,” Jun, 2016. <http://arxiv.org/abs/1606.05908>.
- [40] C. Guo and F. Berkhahn, “Entity Embeddings of Categorical Variables,” [arXiv:1604.06737](https://arxiv.org/abs/1604.06737). <http://arxiv.org/abs/1604.06737>.
- [41] M. Heusel, H. Ramsauer, T. Unterthiner, B. Nessler, and S. Hochreiter, “GANs trained by a two time-scale update rule converge to a local Nash equilibrium,” *Advances in Neural Information Processing Systems 2017-December* no. Nips, (2017) 6627–6638, [arXiv:1706.08500](https://arxiv.org/abs/1706.08500).
- [42] M. Arjovsky, S. Chintala, and L. Bottou, “Wasserstein GAN,” *Proceedings of the 34th International Conference on Machine Learning* **70** (Jan, 2017) 214–223, [arXiv:1701.07875](https://arxiv.org/abs/1701.07875). <https://proceedings.mlr.press/v70/arjovsky17a.htmlhttp://arxiv.org/abs/1701.07875>.
- [43] I. Gulrajani, F. Ahmed, M. Arjovsky, V. Dumoulin, and A. Courville, “Improved training of wasserstein GANs,” *Advances in Neural Information Processing Systems 2017-December* (2017) 5768–5778, [arXiv:1704.00028](https://arxiv.org/abs/1704.00028). <https://github.com/igul222/improved>.
- [44] X. Mao, Q. Li, H. Xie, R. Y. Lau, Z. Wang, and S. P. Smolley, “Least Squares Generative Adversarial Networks,” *Proceedings of the IEEE International Conference on Computer Vision 2017-October* (2017) 2813–2821, [arXiv:1611.04076](https://arxiv.org/abs/1611.04076).
- [45] R. D. Hjelm, A. P. Jacob, T. Che, A. Trischler, K. Cho, and Y. Bengio, “Boundary-seeking generative adversarial networks,” in *6th International Conference on Learning Representations, ICLR 2018 - Conference Track Proceedings*. 2018. [arXiv:1702.08431](https://arxiv.org/abs/1702.08431).
- [46] L. Xu, M. Skoularidou, A. Cuesta-Infante, and K. Veeramachaneni, “Modeling Tabular data using Conditional GAN,” 2019. <http://arxiv.org/abs/1907.00503>.
- [47] P. M. Williams, “Using Neural Networks to Model Conditional Multivariate Densities,” *Neural Computation* **8** no. 4, (1996) 843–854.

- [48] R. Neuneier, F. Hergert, W. Finnoff, and D. Ormoneit, "Estimation of Conditional Densities: A Comparison of Neural Network Approaches," *Icann '94 (1994)* 689–692.
- [49] H. Schioler and P. Kulczycki, "Neural network for estimating conditional distributions," *IEEE Transactions on Neural Networks* **8** no. 5, (1997) 1015–1025.
- [50] L. Prechelt, "Early stopping - But when?," *Lecture Notes in Computer Science (including subseries Lecture Notes in Artificial Intelligence and Lecture Notes in Bioinformatics)* **7700 LECTU** (2012) 53–67.